



Temperature domination of AMOC weakening due to freshwater hosing in two GCMs

Rosalind K. Haskins¹ · Kevin I. C. Oliver¹ · Laura C. Jackson² · Richard A. Wood² · Sybren S. Drijfhout¹

Received: 16 February 2019 / Accepted: 23 September 2019 / Published online: 4 October 2019
© The Author(s) 2019

Abstract

Anthropogenic climate change is projected to lead to a weakening of the Atlantic meridional overturning circulation (AMOC). One of the mechanisms contributing to this is ice melt leading to a freshening of the North Atlantic Ocean. We use two global climate models to investigate the role of temperature and salinity in the weakening of the AMOC resulting from freshwater forcing. This study finds that freshwater hosing reduces the strength of the AMOC, but in some situations it is not through reduced density from freshening, but a reduction in density from subsurface warming. When the freshwater is mixed down it directly reduces the density of the North Atlantic, weakening the strength of the AMOC. As the AMOC weakens, the mixed layer depth reduces and surface properties are less effectively mixed down. A buoyant surface cap forms, blocking atmospheric fluxes. This leads to the development of a warm anomaly beneath the surface cap, which becomes the primary driver of AMOC weakening. We found that the mean North Atlantic salinity anomaly can be used as a proxy for AMOC weakening because it describes the extent of this surface cap.

Keywords AMOC · Thermohaline circulation · Hosing · Density · Model · GCM

1 Introduction

Climate change projections suggest that global warming will cause ice melt and freshening of the North Atlantic Ocean. Paleoclimate research suggests that inputs of large quantities of freshwater have in the past greatly weakened the strength of the Atlantic meridional overturning circulation (AMOC), resulting in far reaching climatic impacts (McManus et al. 2004; Henry et al. 2016). Various simulation studies have shown that forcing the North Atlantic with freshwater reduces the strength of the AMOC (Stouffer et al. 2006; Hawkins et al. 2011). Though freshening is considered to be of secondary importance to radiative forcing in AMOC weakening associated with anthropogenic climate change, the inclusion of ice melt in climate scenarios has

been shown to significantly enhance the AMOC weakening response (Swingedouw and Braconnot 2007; Bakker et al. 2016).

Freshwater forcing studies have been used to investigate the relationship between Atlantic salinity and AMOC weakening. The more freshwater that is added to the North Atlantic, the more buoyant it becomes in comparison to the South Atlantic, reducing overturning by altering the Atlantic meridional density gradient (Cimatoribus et al. 2014; Jackson et al. 2017; Jackson and Wood 2018). The theoretical arguments that underlay AMOC theory (e.g. Bryan 1987; Butler et al. 2016; Sévellec and Huck 2016) indicate that density changes that are confined to the surface have a negligible effect on the AMOC, because thermohaline-led changes to the large scale circulation require perturbations to horizontal pressure gradients over a substantial depth range (Oliver et al. 2005). Therefore it is necessary for the buoyant anomaly to propagate downwards through the water column; which is assumed to occur through the mixing down of freshwater. Questions therefore arise concerning whether the freshwater forcing is increasing buoyancy over a sufficient depth of the North Atlantic in order to directly reduce the strength of overturning, or whether there are intermediate mechanisms involved.

Electronic supplementary material The online version of this article (<https://doi.org/10.1007/s00382-019-04998-5>) contains supplementary material, which is available to authorized users.

✉ Rosalind K. Haskins
rkh1g14@soton.ac.uk

¹ University of Southampton, Southampton, UK

² Met Office Hadley Centre, Exeter, UK

In this study we explore the driving mechanisms of AMOC weakening in response to freshwater forcing. We use two general circulation models (GCMs) to understand the timescales and forcing rates at which different ocean mechanisms become the primary driver of AMOC weakening.

2 Methods and models

2.1 Estimating the AMOC from meridional density gradients

The AMOC can be estimated from a scaling relationship with the meridional density gradient, as discussed in Sijp et al. (2012). This is done by firstly finding the meridional component of the thermal wind equation by taking the vertical derivative of the meridional velocity, using geostrophic balance and the hydrostatic approximation. This gives the basin-scale zonally average meridional velocity, $\langle V \rangle$, as:

$$\frac{\partial \langle V \rangle}{\partial z} = \left(\frac{g}{f_0 \rho_0} \right) \cdot \left(\frac{\Delta \rho_x(z)}{L_x} \right)$$

where g is the gravitation constant, f_0 and ρ_0 are reference values for the Coriolis parameter and density, respectively, $\Delta \rho_x(z)$ is the zonal density difference on each depth level, and L_x gives the zonal length scale.

The next step is to link $\Delta \rho_x$ to the basin-scale meridional density difference, $\Delta \rho_y$. In order to achieve this an assumption of proportionality is made between zonal and meridional velocities (Robinson 1960). This approach was reasoned by Marotzke (1997) as changes in the meridional pressure gradient induce changes in zonal flow, impacting zonal pressure gradients, resulting in changes to meridional flow. The zonal and meridional density differences can then be related using a proportionality factor, n , where $\Delta \rho_x \sim n \Delta \rho_y$. Grouping the constants in the velocity equation above together with n as a scaling factor, c_ρ , then gives the approximation $\langle V \rangle \sim c_\rho \Delta \rho_y H$, where H is the depth scale. Others have attempted to mathematically define a scaling factor between the zonal and meridional density gradients [see discussion in Sijp et al. (2012)]. Approaches which take the mean of the density profile may neglect potentially significant features in the profile structure, becoming distorted by strong anomalies in the surface region. Using the mean of the density profile can yield the qualitatively wrong AMOC response in circumstances where using the depth dependent pressure gradient gives the qualitatively correct response (de Boer et al. 2010). As we are here interested in the physical mechanisms of AMOC weakening, we need to use a method that retains depth dependence in order to be sensitive to processes directly impacting deep pressure gradients. In order to retain the depth dependence of $\Delta \rho_y$

Butler et al. (2016) (hereafter referred to as B16) derived an expression for V :

$$\langle V(z) \rangle = \frac{c_\rho g}{\rho_0 f_0 L_y} \left(\frac{1}{h} \int_{-h}^0 \left(\int_{z'}^0 \Delta \rho_y(z'') dz'' \right) dz' - \int_z^0 \Delta \rho_y(z') dz' \right)$$

where h is the bottom depth. The Atlantic stream function, Ψ , using the vertically integrated meridional velocity in terms of the depth dependent meridional density difference, is then given as:

$$\psi(z) = L_x \int_z^0 \langle V(z') \rangle dz'$$

2.2 Model simulations

Freshwater (hosing) was applied to the surface of the North Atlantic and Arctic region from 50°N to the Bering Strait through a uniform additional surface flux (via a virtual salt flux). We used volume compensation to conserve global volume mean salinity by returning the removed salt to the model evenly through all ocean cells. The hosing remained constant throughout the runs, which continued for between 150 and 250 years. The same experimental design was applied to each simulation, with varying forcing strengths. This experimental design has been previously applied in both of the models used in this study (Jackson and Wood 2018; Haskins et al. 2019), and is used to explore the sensitivity of the AMOC to freshening, and not the fate of the freshwater itself. The northern and southern densities are calculated using full sections of temperature and salinity taken at 50°N and 33°S in the Atlantic. The southern section was placed to describe the densities at the southern limit of the Atlantic Basin while the northern section both captures the subpolar densities and retains sufficient ocean depth to include deep ocean processes. The calculated model AMOC strength is for 30°N. All of these time series are given as the maximum of the stream function over a depth of 200–3000 m.

In this study we have used two distinct models, with component parts of different provenance, in order to avoid model dependent conclusions. Firstly, the eddy-permitting GCM HadGEM3-GC2 (Williams et al. 2015), that combines the Global Ocean v5 model from NEMO (Megann et al. 2014) with the Global Atmosphere v6 model of the Met Office UM. There are 75 levels in the ocean, with resolution 0.25°, and 85 levels in the atmosphere with a resolution of ~135 km at mid-latitudes. We used hosing rates of 0.1, 0.2, 0.3 and 0.5 Sv [see Jackson and Wood (2018) for more description of these experiments]. The HadGEM3-GC2 control run has a steady AMOC strength of ~14 Sv, with linear drifts in temperature and salinity in the north and south of the Atlantic. The control run has constant pre-industrial forcing applied

and has been spun up for 146 years (after initialisation from a previous present day control run). Although there is little drift in the upper ocean and in the AMOC strength, deep ocean properties have not had time to reach equilibrium. In the control run, the density changes in the south appear to strengthen the AMOC and the north appears to weaken it, both by 1 Sv per 100 years, Fig. 1. This is due to a basin-wide negative drift in deep density, which has little effect on the reconstructed AMOC, but does affect its decompositions into northern and southern components. As the strengths of these drifts are dependent upon the state of the ocean we do not remove linear trends from the experiments, but instead consider the results in the light of these drifts. We would expect the ocean state to change more in the North Atlantic than in the South Atlantic in response to the freshwater hosing, and therefore, for the density drift to be more strongly altered in the north than in the south.

Our second model is the Fast Met Office/UK Universities Simulator ‘FAMOUS’ (Smith et al. 2008; Smith 2012), which is a computationally cheaper version of HadCM3 (Gordon et al. 2000). FAMOUS comprises the Hadley Ocean model (HadOM3), which is unrelated to the NEMO ocean used in HadGEM, and the Hadley Atmosphere model (HadAM3). The ocean has 20 levels, with resolution 3.75° by 2.5° , and the atmosphere has 11 levels of 7.5° by 5° . The model is not eddy-permitting and so uses the Gent-McWilliams scheme (Gent and McWilliams 1990). Due to the lower resolution, we are able to use a 1000-year spin-up followed by an ensemble approach with 10 run at each hosing rate. The FAMOUS control run has an AMOC strength

of 17.5 Sv, and shows no drift in AMOC, salinity, or temperature. As there is a simple relationship between hosing and model response in FAMOUS, we will only present runs hosed with 0.2 and 0.5 Sv of freshwater. These experiments were previously described in Haskins et al. (2019).

3 AMOC behaviour and reconstruction

In both models the freshwater input collects at the surface of the hosing region, with changes in ocean transports unable to dissipate the anomaly at the rate of input. In both models, freshwater hosing leads to a reduction in the strength of the AMOC, Fig. 2, left axis. The total extent of AMOC weakening in FAMOUS is larger with greater hosing rates, while all hosing rates in HadGEM3-GC2 ended within a couple of Sverdrup of each other [<4 Sv, see Jackson and Wood (2018)]. Unlike HadGEM3-GC2, FAMOUS saw a strengthening of the Antarctic Bottom Water (AABW) cell (not shown). HadGEM3-GC2 shows greater interannual variability than FAMOUS. Due to the differences in control strength between the two models, we cannot directly compare their behaviour in terms of magnitude of deviation.

The B16 method is able to reconstruct the primary form of AMOC weakening for all runs Fig. 2. However, as the output is scaled to match the model mean control run strength, the method does not capture the extent of AMOC weakening. For our purposes this is not important, as we are interested in the underlying mechanisms and not the magnitudes of AMOC strength.

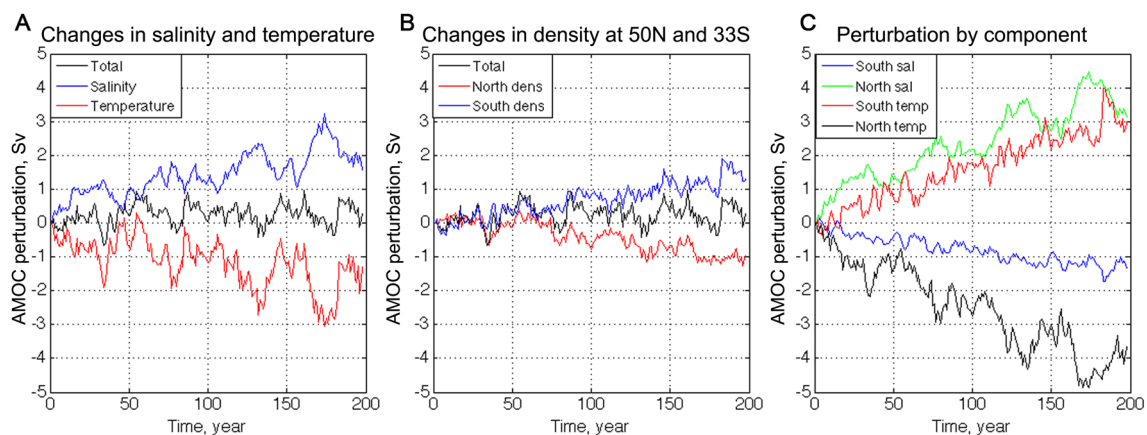
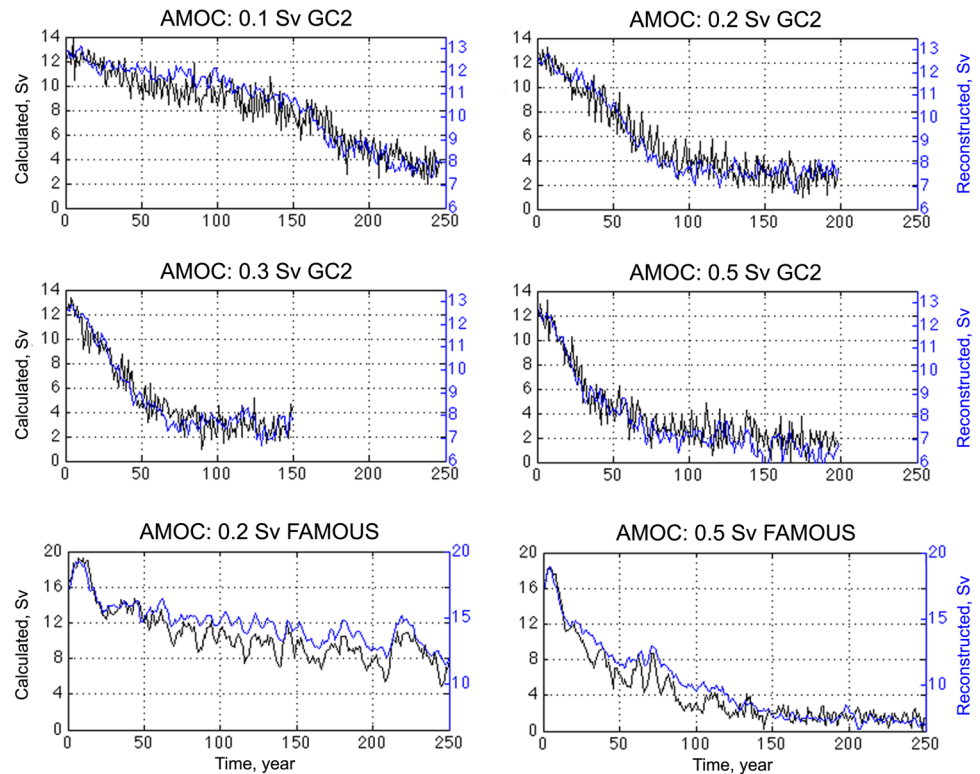


Fig. 1 Perturbation in AMOC strength (Sv) due to model drift in northern and southern temperature and salinity, as reconstructed using the Butler et al. (2016) method. The panels split the influence on AMOC perturbation between that from a changes in north–south

difference in salinity and temperature, b density changes occurring in the north and south of the Atlantic, and c each of these four components (southern salinity, northern salinity, southern temperature, northern temperature)

Fig. 2 Left Y-axis AMOC as calculated from the model velocities. Right Y-axis AMOC as reconstructed using the Butler et al. (2016) method. All panels show annual data for a single run, with the HadGEM3-GC2 (labelled GC2) data having greater variability. The magnitude of weakening is underestimated by the reconstruction. Note that different left and right Y-axis scales have been used



4 Role of temperature and salinity in AMOC changes

We want to understand the relative influence of temperature and salinity in the north and south of the Atlantic on the weakening of the AMOC. We use the same method to reconstruct the AMOC, while isolating the AMOC perturbation resulting from each component by holding all other profiles constant at the first timestep. This is first split between the AMOC perturbation resulting from density changes at 50°N and 33°S, Fig. 3a. In all simulations the AMOC weakens due to changes in density in the north. The density changes in the south modulated the overall weakening. These roles in the north and south were identified in FAMOUS by Haskins et al. (2019), and the present study shows similar behaviour in an eddy-permitting model.

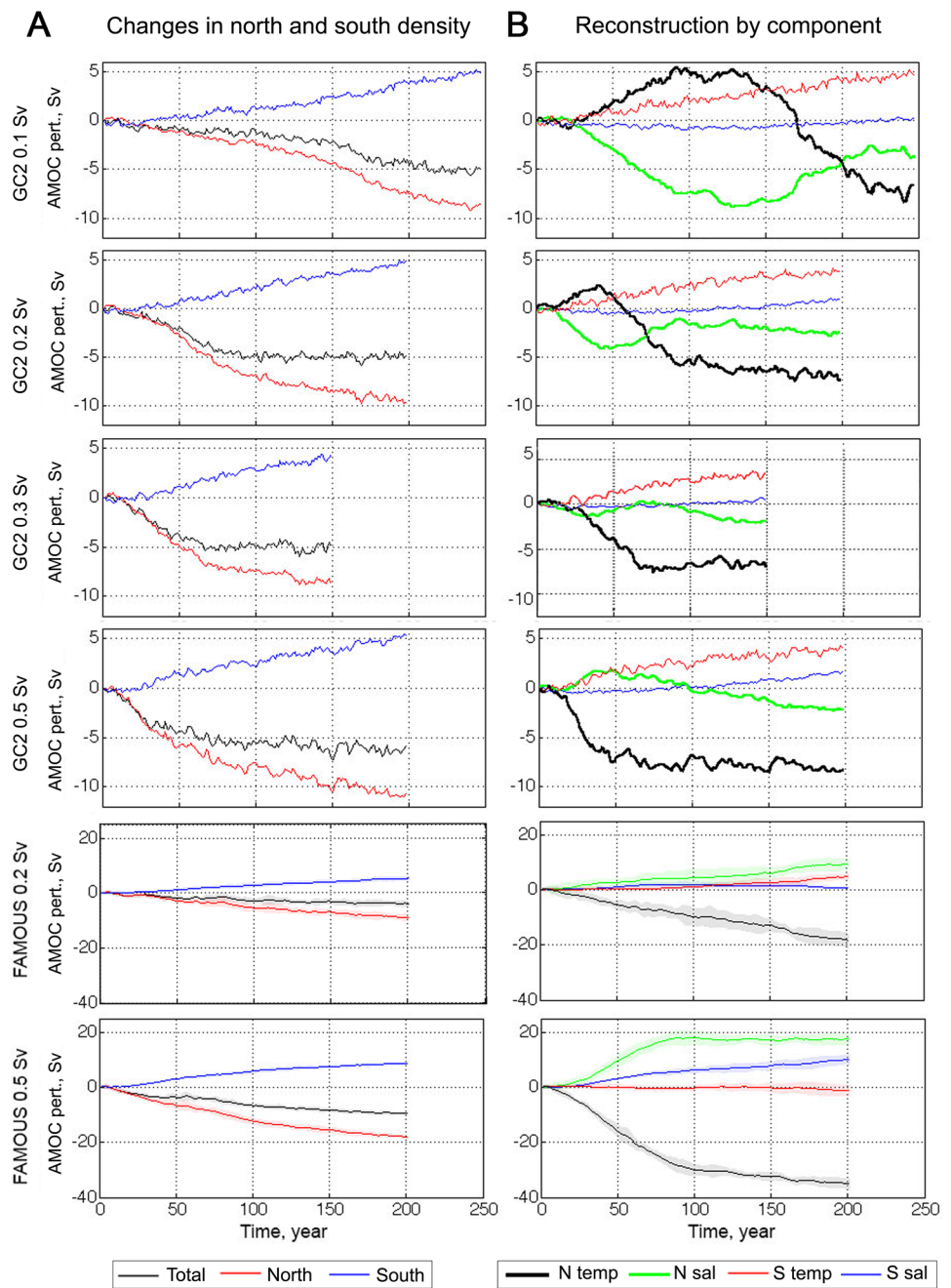
The density in the north and south is then split into the AMOC perturbation driven by changes in temperature and salinity, Fig. 3b. In all runs northern temperature ultimately gives the greatest contribution to weakening the AMOC, even though the weakening is driven by freshwater hosing. In the HadGEM3-GC2 runs, with modest hosing the initial AMOC weakening is driven by changes in northern salinity, but the salinity driven perturbation then diminished and is overcome by the effect of the northern temperature. The greater the hosing rate the sooner temperature dominates the AMOC weakening. The relationship between the AMOC perturbations from

temperature and salinity changes shows a progression with increasing hosing rates. The first 200 years of hosing at 0.1 Sv shows a similar pattern to the first 75 years of hosing at 0.2 Sv. In the 0.3 and 0.5 Sv runs weakening from temperature exceeds salinity after the first 30 and 20 years, respectively. If the control run model drifts were removed from these results, the AMOC perturbations from northern temperature and salinity on weakening the AMOC would have been weaker and stronger, respectively (see Supplementary Materials), reducing the extent of temperature domination.

In FAMOUS, northern temperature changes weaken the AMOC, while the northern salinity changes enhance the AMOC. This dynamic is consistent from the beginning, at both hosing rates. With stronger hosing, the magnitude of AMOC perturbation is greater, and levels off as the AMOC becomes very weak (~ 3 Sv in Fig. 2).

Density changes in the south strengthened the AMOC in all runs. However, this was achieved by different mechanisms in the two models. In all of the HadGEM3-GC2 runs the southern temperature gave a near linearly increasing AMOC enhancement, this is likely significantly contributed to by the South Atlantic warming temperature drift in the model. In FAMOUS, the southern AMOC enhancement was driven by different components for the two hosing rates. With stronger hosing rates (0.3 Sv and above) it is driven by reduced salinity.

Fig. 3 **a** Reconstruction of AMOC strength, presented in terms of AMOC perturbation resultant from changes in the density profiles at 50°N (red), 33°S (blue) and total (black). **b** Reconstruction of AMOC perturbation from changes in density profiles due to changes in temperature and salinity at 50°N and 33°S. The Y-axes vary by model. The HadGEM3-GC2 (labelled GC2) results are for single model runs. The FAMOUS panels show the 10-member ensemble mean, with standard deviation shaded



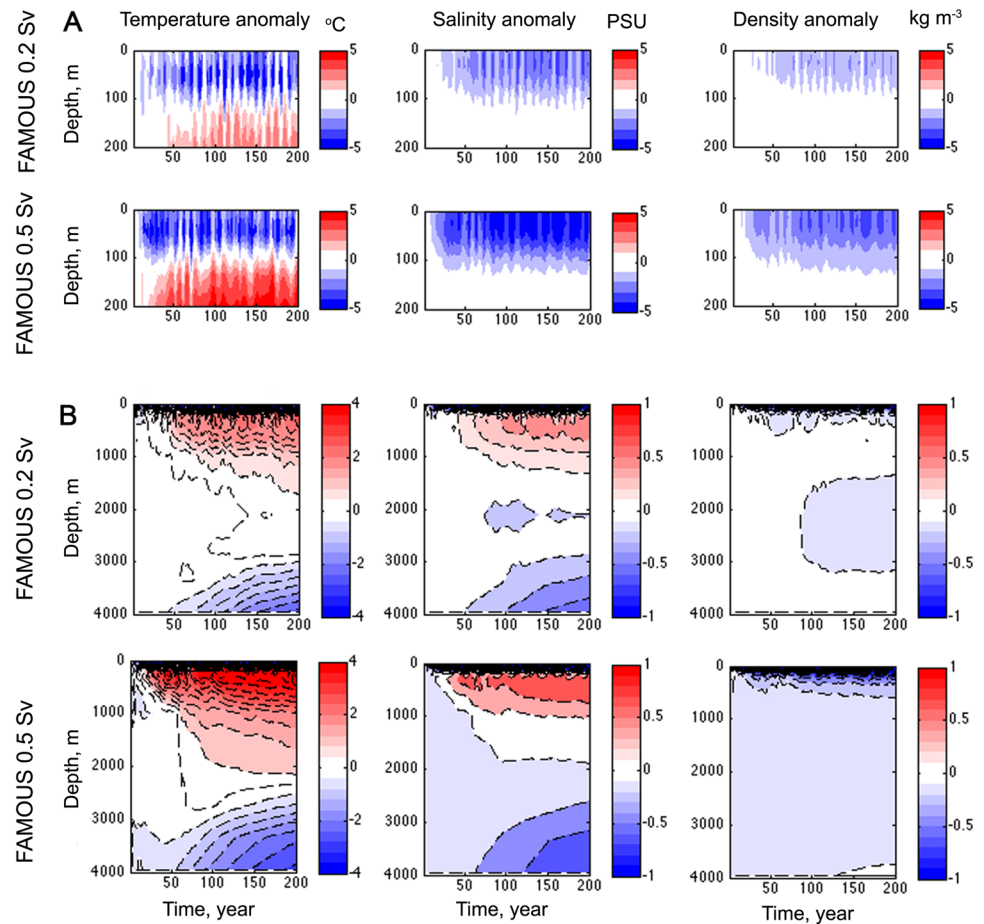
5 Mechanisms of AMOC weakening in the North Atlantic

The AMOC reconstructions by component suggest that to understand the primary mechanisms of AMOC weakening it is sufficient to understand the behaviour of temperature and salinity at 50°N, and their impacts on density. We will first explore the relatively simple mechanisms in FAMOUS and then examine the more complex response in HadGEM3-GC2.

5.1 Mechanisms in FAMOUS

AMOC weakening in response to freshwater hosing in FAMOUS is invariably driven by warming at 50°N, Fig. 3. In order to understand why this is, we will consider the temporal variations in the profiles of temperature and salinity at 50°N, Fig. 4. In this description, the first values stated are for the 0.5 Sv 10-member ensemble mean, with the 0.2 Sv ensemble mean value in brackets.

Fig. 4 Hovmoller anomaly (from first time-step) plots showing the FAMOUS 10-member ensemble mean for temperature ($^{\circ}\text{C}$) salinity (PSU) and calculated density (kg m^{-3}) at 50°N in the Atlantic. **a** shows the formation of the surface cap in the top 200 m, **b** shows the full depth. Note different colour scale in **a** and **b**



As a result of hosing a 100 m deep fresh cap is established at the surface Fig. 4a, with a final salinity anomaly of -5 PSU (-2.5 PSU). The surface cap shows strong cooling, by -4 $^{\circ}\text{C}$ (-3 $^{\circ}\text{C}$). Below the surface cap (200–2000 m) Fig. 4b, the ensembles have warm, saline, anomalies reaching 4.5 $^{\circ}\text{C}$ (2.5 $^{\circ}\text{C}$) and 0.8 PSU (0.5 PSU). These warm waters are isolated from the atmosphere by the surface cap, which reduces heat loss to the atmosphere and traps in the heat transported into the region by the ocean (see Haskins et al. 2019 for more detail). Below 2000 m a cold fresh anomaly develops more slowly, reaching a maximum magnitude of -2.5 $^{\circ}\text{C}$ (in both ensembles) and -0.6 PSU (-0.5 PSU) at greatest depth. This signal results from the intrusion of the strengthened AABW (not shown).

To understand the net impact of these changes we look at the resultant changes in density at 50°N . Both ensemble means develop a low-density cap within the surface 100 m (-3 kg m^{-3} for the 0.5 Sv ensemble), with the impact of freshening outweighing the impact of cooling. However, a more dynamically important change in density comes from subsurface warming. The warming reduces densities through ~ 2000 m of the water column, giving a particularly strong low-density anomaly to a depth of 500 m.

With increasing depth, warm saline anomalies give way to cool fresh anomalies, associated with the extension of the AABW, giving little change to the net density.

In FAMOUS the AMOC is weakened by the high temperature anomaly that develops under the buoyant surface cap, due to the reduction in the surface heat flux. The reconstruction shows that the salinity at 50°N enhanced the AMOC despite the freshwater hosing. This has been shown to result from an increased ocean salinity convergence in FAMOUS, with an increase in salinity in the waters transported into the region (Haskins et al. 2019). The increased northward salinity transport at 50°N is caused by changes in the low latitude North Atlantic surface freshwater fluxes (see Fig. 8). These arise from changes in atmospheric circulation patterns, notably the southward shift of the Intertropical Convergence Zone, during weak AMOC (Wu et al. 2011; Jackson 2013; Bouttes et al. 2015; Haskins et al. 2019). While there is surface freshening, the major influence from salinity is the high salinity anomaly from 200 to 2000 m, increasing North Atlantic density and thereby enhancing the strength of the AMOC.

5.2 Impact of salinity and temperature on density at 50°N in HadGEM3-GC2

HadGEM3-GC2 had a more complex response to hosing, with initial AMOC weakening dominated by North Atlantic freshening. However, with greater quantities of hosing, temperature eventually dominated AMOC weakening, showing similar behaviour to that seen in FAMOUS. In order to understand the behaviour of HadGEM3-GC2, we will again begin by considering the temporal variations in the profiles of temperature, salinity and calculated density at 50°N, Figs. 5 and 6.

The model responds to relatively modest hosing with surface freshening Fig. 5, which extends its vertical distribution with time, and a reduction in subsurface temperatures, consistent with reduced northward heat transport. However, as the quantity of freshwater hosing increases, we again see the development of a fresh surface cap (with a salinity anomaly of -3.5 PSU for the 0.5 Sv run). This anomaly takes longer to establish for lower hosing rates, forming in 30 years in the 0.5 Sv run and 200 years in the 0.1 Sv run. All runs develop a strong cold anomaly within the surface cap, which is stronger for the 0.5 Sv run in HadGEM3-GC2 than it was in FAMOUS (-5 °C compared to -4 °C).

Below the surface cap we see a warm anomaly develop in all runs Fig. 6, which is weaker (2.5 °C for the 0.5 Sv run) in HadGEM3-GC2 than it was in FAMOUS. The temperature anomaly reaches greater depths, and extends downwards faster in HadGEM3-GC2 than in FAMOUS. There is a double-dip in subsurface salinity, where the initial freshening partly recovers, and later again freshens (not seen in the 0.1 Sv experiment, where only one dip is present within the experiment duration). The initial freshening is deeper, and longer lasting, for weaker hosing rates. There is a weak cool anomaly, with some freshening, between 2500 and 3000 m (-0.7 °C for the 0.5 Sv run) consistent with AMOC shoaling.

All net density changes at 50°N are negative, with stronger hosing giving greater reductions in density. While freshening does reduce subsurface North Atlantic density during times of salinity domination in HadGEM3-GC2, the density anomaly is much weaker than that present during times of temperature domination. All runs eventually develop a low-density cap within the surface 100 m, with the impact of freshening outweighing the impact of cooling Fig. 5. Below this density is reduced by subsurface warming between depths of 200 and 1500 m, developing under the surface cap Fig. 6. The deep (~ 3000 m) cooling is balanced by freshening, giving no significant change in net density.

Fig. 5 Hovmoller anomaly (from first time-step) plots showing the temperature (°C) salinity (PSU) and calculated density (kg m^{-3}) of the top 200 m at 50°N in the Atlantic for each hosing rate in HadGEM3-GC2. The same colour bar limits have been applied throughout. Black vertical marks the end of simulation

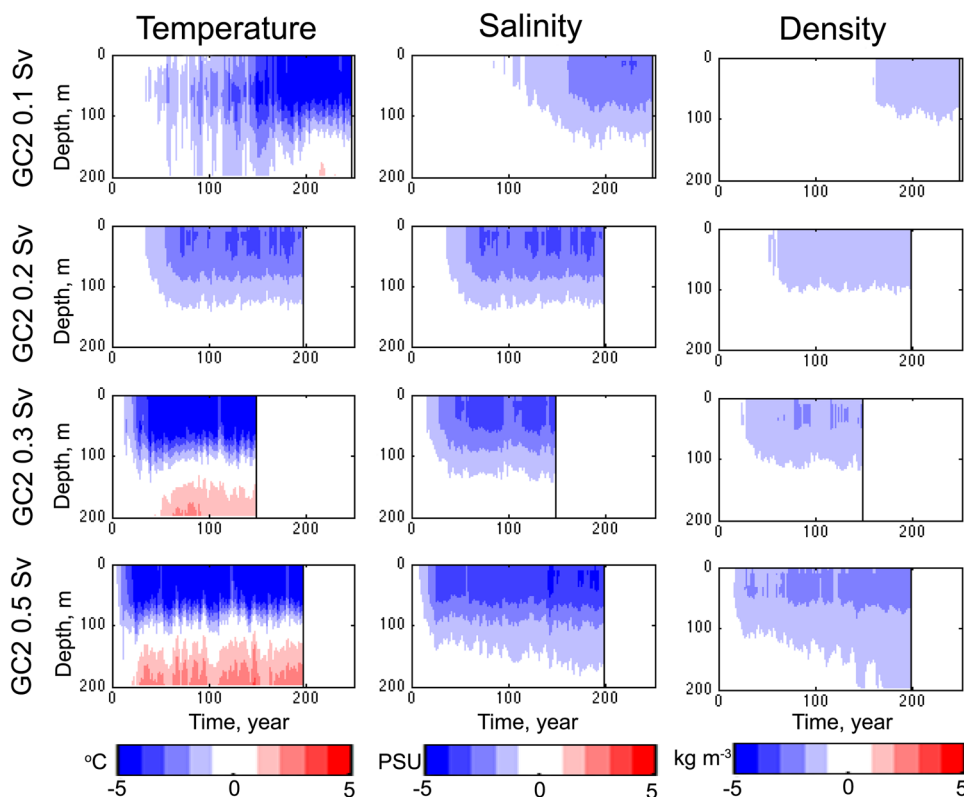
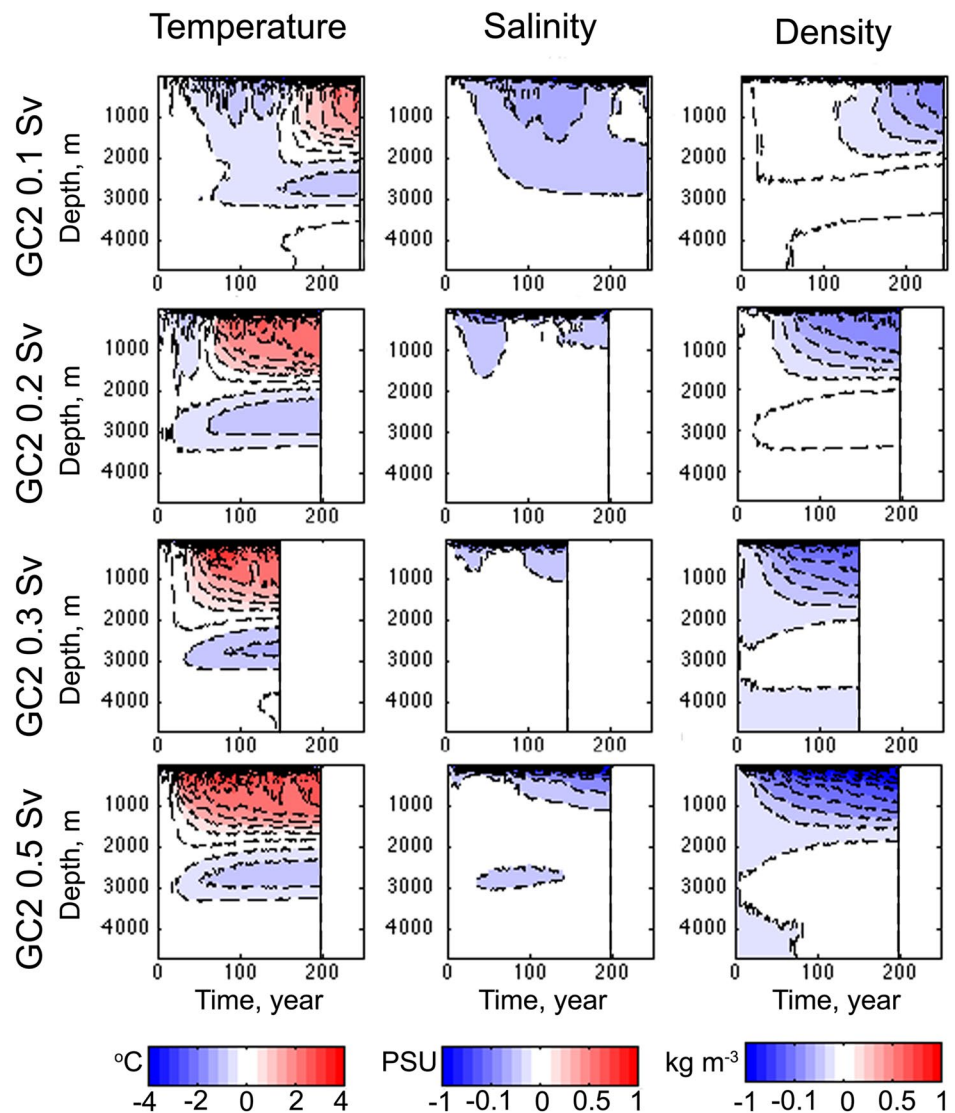


Fig. 6 Hovmoller anomaly (from first time-step) plots showing the full depth temperature ($^{\circ}\text{C}$) salinity (PSU) and calculated density (kg m^{-3}) at 50°N in the Atlantic for each hosing rate in HadGEM3-GC2. The same colour bar limits have been applied throughout. Black vertical marks the end of simulation



5.3 Ocean mechanisms and feedbacks on density in HadGEM3-GC2

The time taken for temperature at 50°N to dominate AMOC weakening is related to the time taken to establish a surface cap, trapping in a heat anomaly. In HadGEM3-GC2, as the AMOC weakens the depth of the March Labrador Sea mixed layer depth (MLD) reduces and becomes steady at ~ 140 m, reducing convection, Fig. 7. Within the mixed layer there are low-density highly buoyant waters, with the cool fresh anomaly becoming isolated at the surface. The surface fluxes over a 10° band centred on 50°N , Fig. 7, show that the ocean ceases to release net warmth to the atmosphere. The net freshwater surface flux into the same region of the ocean increases during hosing, as reduced northward ocean heat transport leads to surface cooling and reduced evaporation. Therefore, the change in both heat and freshwater surface fluxes act to increase

the buoyancy of the surface cap and feed the buoyancy reservoir.

The surface freshwater fluxes over the North Atlantic and Arctic are broadly intensified, Fig. 8. Initially, the region north of the tropics in the Atlantic net received freshwater from the atmosphere, while the Arctic net exported freshwater at the ocean surface—primarily to the formation of high-latitude ice. In the final decade of the 0.5 Sv hosed run both of these fluxes had become stronger. The North Atlantic, into the Greenland, Iceland and Norwegian (GIN) seas, usually gives off heat to the atmosphere. As the AMOC weakens, the surface heat flux is strongly reduced from 30°N to high latitudes, including a horseshoe shaped reduction in ocean heat loss in the North Atlantic, associated with periods of weak AMOC. Hence the surface flux changes we see at 50°N in Fig. 7 are representative of wider changes to the surface fluxes in the sub-polar region.

Fig. 7 March Labrador Sea MLD (m), upward surface freshwater flux (including net evaporation and sea ice processes) (kg s^{-1}), and the upward surface heat flux (W). Both surface fluxes are 10-year rolling means integrated over a Section 45–55°N, over the full width of the North Atlantic. All data is for HadGEM3-GC2. Hosing is not included in the freshwater flux. The legend applies to all panels

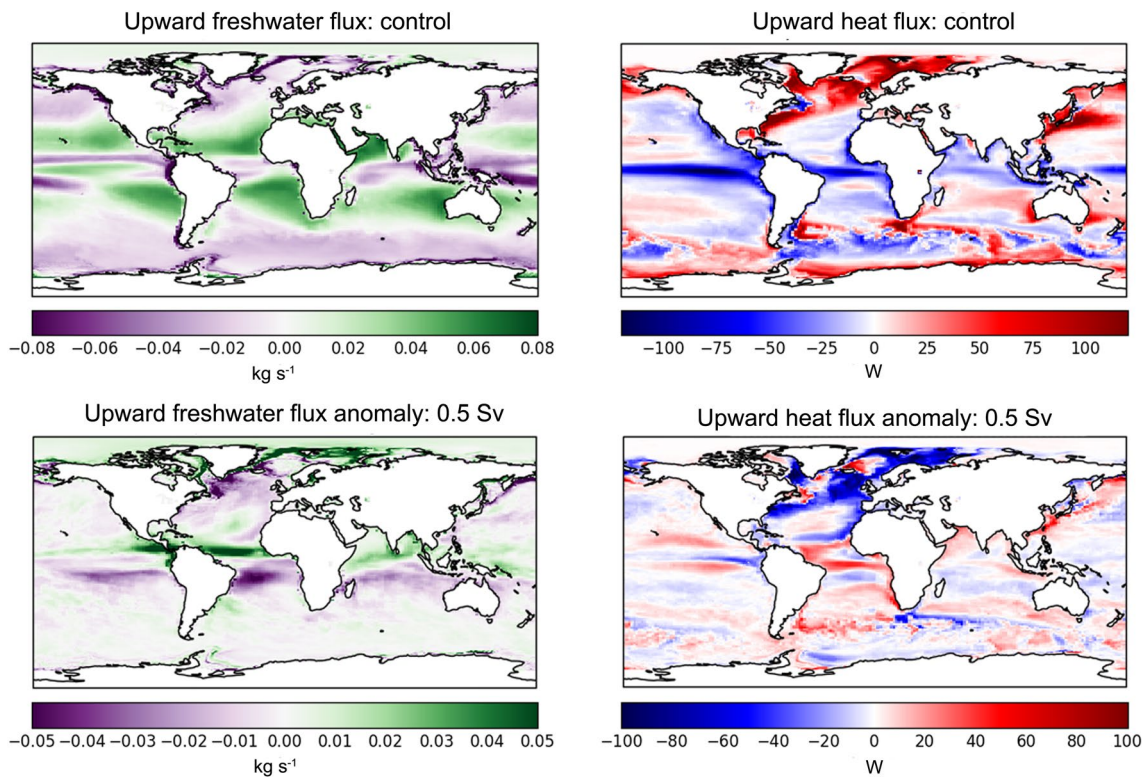
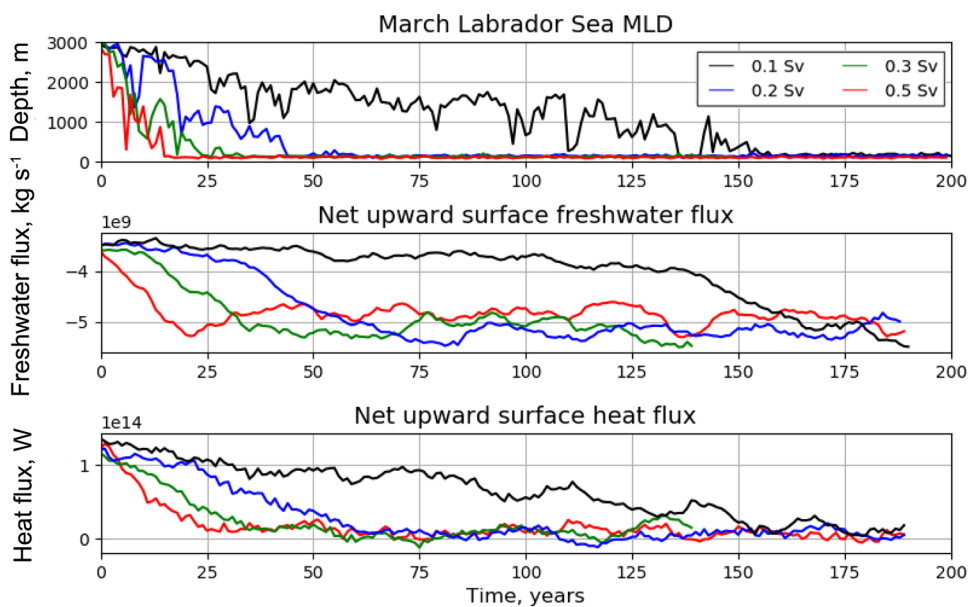
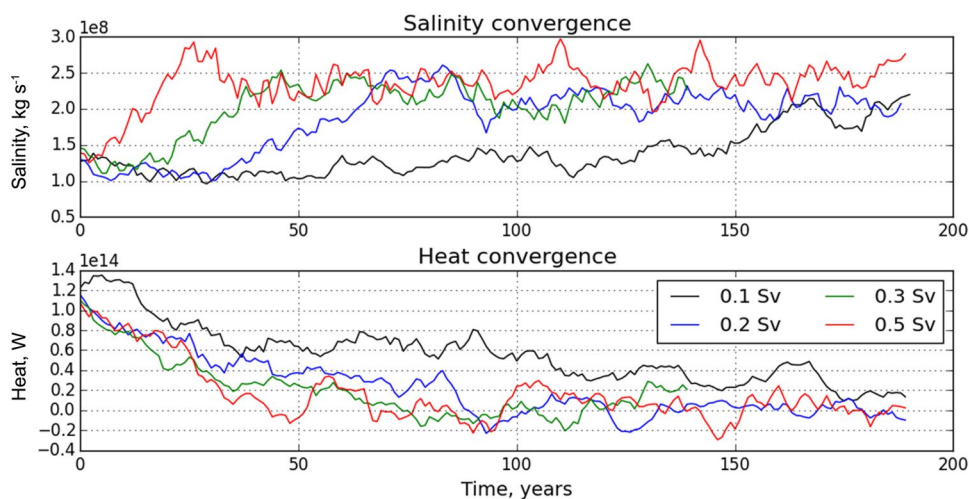


Fig. 8 Decadal mean upward surface freshwater flux (including net evaporation and sea ice processes) ($\text{kg m}^{-2} \text{s}^{-1}$) and upward surface heat flux (W m^{-2}) for the control run (top) and the anomaly at the end of the 0.5 Sv hosed run (lower)

Changes in northward transport of heat and salinity both act to increase the density at 50°N, Fig. 9. As the AMOC weakens, salinity convergence from 45 to 55°N due to ocean transport is increased, leading to the temporary reduction of subsurface salinity anomalies seen in Fig. 6 (years 80–120

and 50–100 in the 0.2 Sv and 0.3 Sv runs, respectively). The heat convergence over the same area reduces as the AMOC weakens. This is lead by reduced northward heat transport at 45°N (not shown), and is seen in the early cooling Fig. 6. However with further hosing, the warmth

Fig. 9 Convergences in northward ocean transports of salinity (kg s^{-1}) and heat (W), for a 10° region over 50°N in the Atlantic in HadGEM3-GC2. A 10-year rolling mean has been applied. Legend applies to both panels



previously exported to the atmosphere is trapped below the surface cap, causing subsurface warming. If surface fluxes had remained constant, then changes in ocean heat convergence alone would have given further cooling. Changes in both salt and heat advection therefore act to increase the density and oppose AMOC weakening.

5.4 Attributing dominance in HadGEM3-GC2

The pattern in reconstructed AMOC strength due to changes in northern salinity and temperature in HadGEM3-GC2 is simpler when considered in terms of the total freshwater added, Fig. 10a, b. The AMOC changes little during the first 2.5 Sv yrs of hosing (e.g. 25 years at 0.1 Sv or 5 years at 0.5 Sv), but after this it is weakened by salinity changes. This is due to the early freshwater input being mixed downwards by the continuing overturning, reducing the densities down through the water column. The initial AMOC strengthening by temperature, Fig. 10b, in the HadGEM3-GC2 0.1 and 0.2 Sv runs is due to the reduced northward transport of heat throughout the AMOC depth, which leads to a cooling up to years 150 and 70, respectively, Fig. 6. This is not seen in the heavier hosed runs as they have less time to be impacted by this cooling mechanism before reductions in the surface heat flux cause a more significant warming. The weaker hosing rates have larger anomalies in temperature and salinity, however these largely compensate giving relatively weak net AMOC change.

Both the AMOC enhancement by the temperature contribution and AMOC weakening by the salinity contribution start to decline after ~ 10 Sv yrs of hosing—with the transition occurring earlier for more heavily hosed runs. In the 0.5 Sv run, the AMOC weakening due to subsurface warming is partly moderated by increased salinity. The AMOC enhancement from salinity is caused by the subsurface salinity increasing, in the middle of the freshening double-dip, as

the AMOC is strengthened by increased salinity convergence by ocean transports at 50°N , Fig. 9. Note that changes in the behaviour and influence of temperature and salinity are not apparent in the linear relationship between AMOC strength and total freshwater added Fig. 10c—suggesting that the AMOC is not sensitive to whether the salinity or temperature dominates the weakening.

After 20 Sv years, the linear relationship between model AMOC weakening and total freshwater input breaks down, Fig. 10c. The impact of northern temperature change on AMOC strength largely levels off while there is still some weakening from salinity change at 50°N .

6 How does using the volume mean density method compare?

Previous studies (i.e. Jackson and Wood 2018) have estimated AMOC strength using the difference in the volume mean density between the north and south of the Atlantic, and found AMOC weakening to be dominated by the buoyancy impact of the salinity in the North Atlantic. In order to compare the two approaches, we have estimated the AMOC from the difference in the vertical mean of the density profiles at 50°N and 33°S for the HadGEM3-GC2 runs, and repeated the above component analysis, Fig. 11. Here the 'volume' used is the full depth and width of the basin, taken over 1 latitudinal cell, which we consider representative of densities local to 50°N and 33°S , while allowing us to use the same temperature and salinity time series as in the previous method.

In our experiments, the estimated AMOC from the vertical mean density gives a good approximation to the form of the model AMOC. The breakdown by component suggests domination by northern salinity, with a later contribution by temperature. The higher the hosing rate,

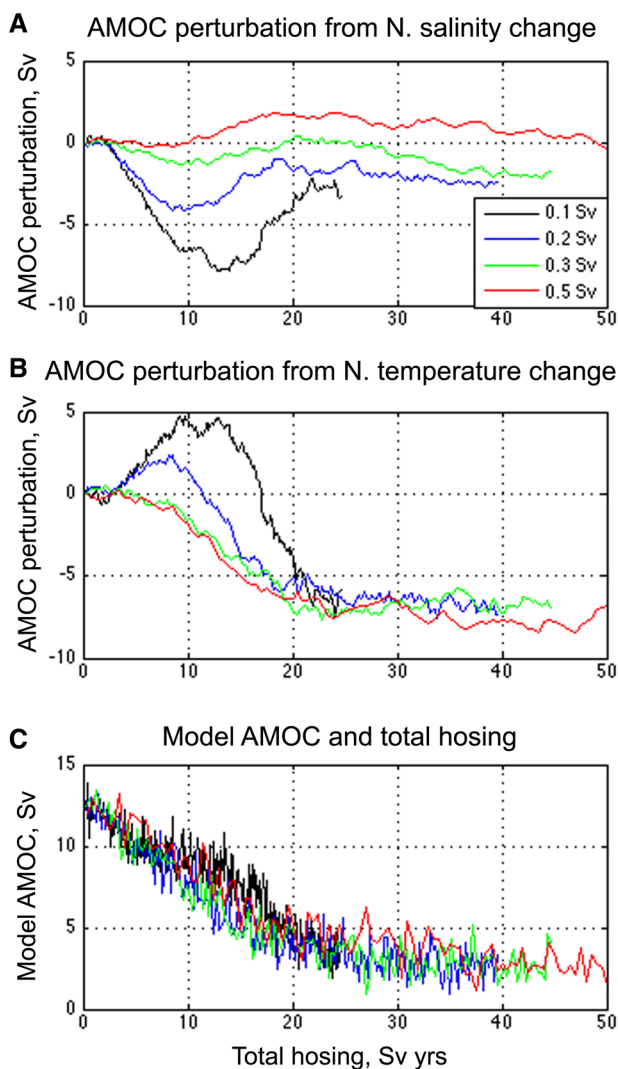


Fig. 10 **a** AMOC perturbation (Sv) from changes in salinity at 50°N (green line on Fig. 3b) against cumulative freshwater input. **b** AMOC perturbation (Sv) from changes in temperature at 50°N (black line on Fig. 3b) against cumulative freshwater input. **c** Model AMOC strength (Sv) against total freshwater hosed (Sv year). All data is for HadGEM3-GC2, up to a maximum of 50 Sv years. Legend applies to all panels

the faster and greater the contribution from northern temperature change becomes to AMOC weakening, becoming temporarily comparable with the salinity contribution for the 0.5 Sv experiment through years 40–100. Using the volume mean approach, the northern salinity contribution includes time series features that are qualitatively similar to those seen in the B16 method's analysis. Here the salinity has an additional weakening trend on the AMOC strength due to the volume mean method's greater sensitivity to surface freshening. The AMOC perturbation from the northern temperature has similar form, with a weaker signal, to the results found using the B16 method. The

role of density in the South Atlantic is similar between methods.

To understand why the two methods give different results we consider the weighting each gives to different processes in the density profile. The volume mean density approach takes the vertical mean value of the profiles, and so changes may be dominated by the very strong surface salinity anomalies within the surface cap. The B16 method uses a double integration up the water column, and so places greater emphasis on changes at deeper levels within the ocean.

The impact of changes in northern salinity on AMOC strength using the volume mean approach, Fig. 11, appears to primarily represent the development of a fresh surface cap. We can approximately recreate the form of the northern salinity contribution from the mean salinity of the top 60 m at 50°N, Fig. 12a. However, the form of the salinity contributions using the B16 method, Fig. 3b, show a closer correlation to the mean salinity through 180–4700 m, Fig. 12b. This can be understood as the full depth mean salinity being disproportionately impacted by strong surface anomalies, Fig. 12c, which cannot drive large transport anomalies without being propagated to a greater depth.

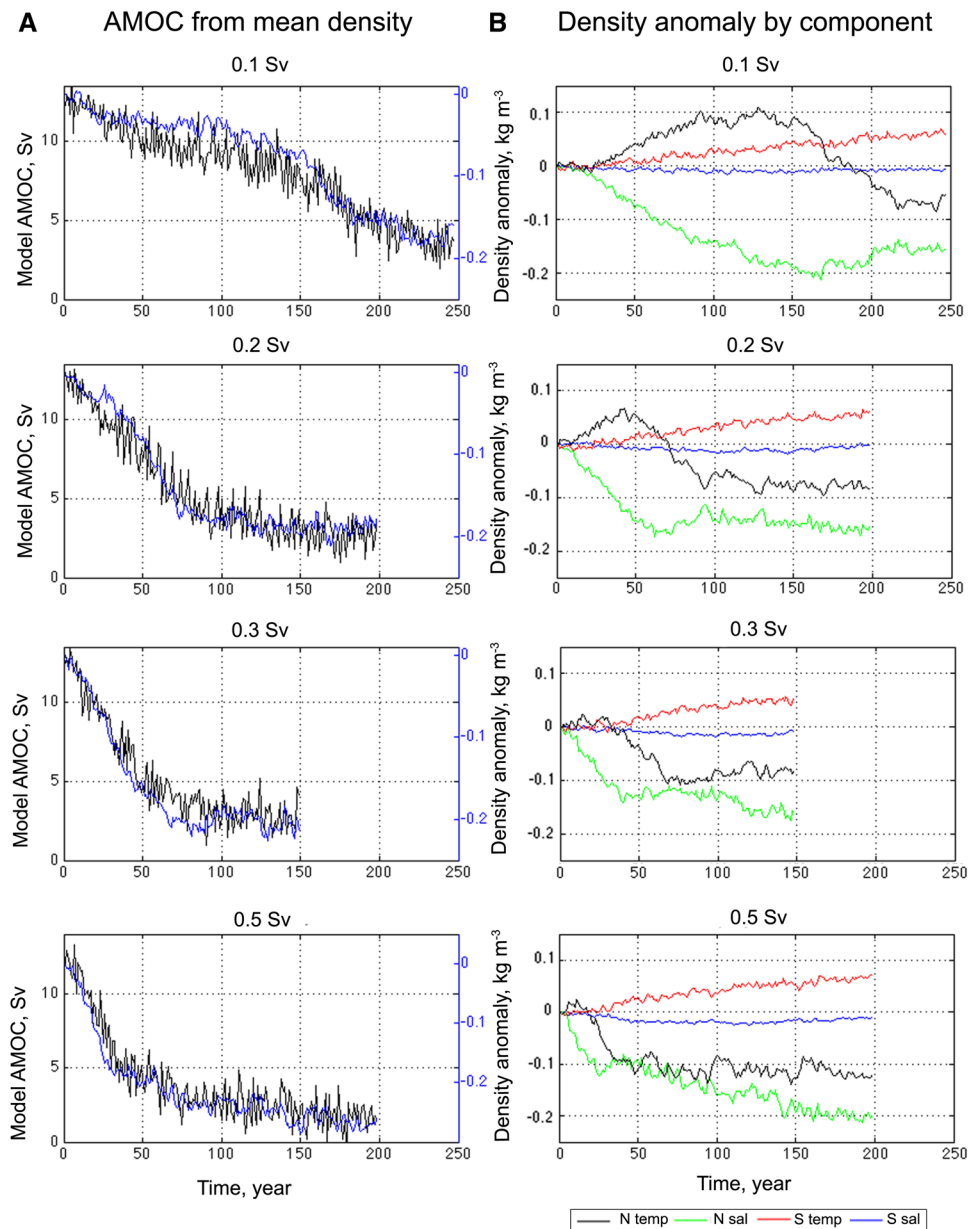
We are postulating that the mean North Atlantic salinity anomaly acts as a proxy for AMOC weakening because it describes the extent of the surface cap. However, once the cap is formed the AMOC is not reduced directly by the buoyancy of this freshwater. We find that AMOC weakening is instead driven by increases in subsurface temperature as a consequence of reduced surface heat loss. This is caused by the freshwater cap limiting convection and isolating the subsurface water from the atmosphere.

7 Discussion

At the onset of hosing in the HadGEM3-GC2 hosing simulations, the freshwater is transported downwards by the AMOC, reducing the density through a significant depth of the water column and thereby reducing the strength of the AMOC. The mixed layer shoals, which reduces the mixing down of surface properties, enabling the formation of a fresh surface cap. The surface cap acts as a barrier between the subsurface ocean and atmosphere, preventing the warm northward ocean transports from being able to release their heat, causing a warm temperature anomaly to develop beneath the cap. The heat anomaly further reduces the density of the ocean. In all of our simulations, the temperature contribution eventually dominates over salinity in driving AMOC decline in response to freshwater hosing.

Both the depth-dependent method and the volume mean density approach were able to reconstruct the strength of the AMOC. However, the volume mean density approach gave greater perturbation to AMOC strength from changes

Fig. 11 **a** Comparison of model AMOC strength (Sv) and the estimated form of AMOC change from the anomaly in meridional density difference (kg m^{-3}) calculated from the volume mean density at 50°N and 33°S in the Atlantic. Here, the ‘volume’ is the full depth and width of the basin, taken over 1 latitudinal cell. **b** Anomaly in meridional density difference (kg m^{-3}) from changes in temperature and salinity at 50°N and 33°S



in North Atlantic salinity, since the volume mean values give equal weightings to density changes at the surface and at depth and hence were dominated by strong surface anomalies. The depth-dependent method showed greater temperature dominance of AMOC weakening, as it was more responsive to dynamically important variations in pressure gradients at depth, where temperature changes dominate. AMOC theory suggests that surface anomalies are not directly dynamically significant in determining the strength of the AMOC and that the depth-dependent method is a more theoretically sound technique for identifying the physical mechanisms of AMOC weakening (Oliver et al. 2005; de Boer et al. 2010). In our experiments the volume mean approach acts as a proxy by indicating

the extent of the fresh surface cap, which is well correlated with AMOC decline. This suggests that while the volume mean approach can be used to reconstruct the AMOC and can be used alongside density budget analysis, understanding the vertical distribution of density changes is also important.

Previous freshwater forcing studies have also found high latitude subsurface temperature increase to result from suppression of ventilation, destabilising the water column (Mignot et al. 2007; Krebs and Timmermann 2007). Our work indicates that this temperature anomaly is not merely a by-product of the hosing, but is the dominant mechanism by which the AMOC is weakened in response to strong and/or long-term hosing.

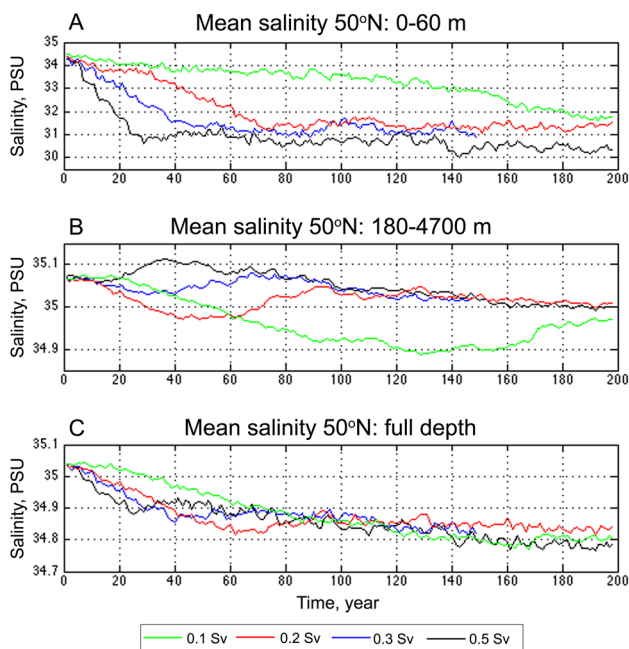


Fig. 12 Volume mean salinity (PSU) over a box 45–55°N over the full width of the Atlantic for the HadGEM3-GC2 runs. **a** from 0 to 60 m, **b** 180–4700 m, and **c** the full depth. Legend applies to all plots

For the weakest hosing rates examined, which are more relevant for past and future climate change, this study suggests that salinity would initially dominate AMOC weakening, and that tracking the depth of the MLD could be used as an indicator of mechanistic change, after which heat would dominate. In climate change scenarios forced with radiative forcing, which allow for Greenland ice mass loss, the weakening of the AMOC has been suggested to be dominated 60% by changes in North Atlantic temperature, 40% by salinity (Thorpe et al. 2001). In such simulations the AMOC is primarily weakened by thermally stratifying the upper ocean. This study has suggested that the formation of a surface cap in response to surface freshening may also contribute to North Atlantic subsurface warming. This suggests that both hosing and radiative forcing ultimately act in the same way, by preventing heat loss from the subsurface North Atlantic. It is unclear how these two forcing mechanisms would interact, whether later local surface heating would be mixed down to the upper ocean, impacting AMOC strength, or whether it would remain above the shallow MLD reinforcing the isolation of a warm and fresh surface cap, and preventing AMOC recovery. Either way, in terms of AMOC weakening they may be expected to reinforce rather than mitigate each other.

An interesting result of this study is that freshwater forcing can result in a weakening of the AMOC whether or not the freshwater propagates down the water column. When the freshwater does mix downwards, the increased buoyancy

of the freshened region leads to AMOC weakening. While freshwater that does not mix downwards collects to form a barrier to surface fluxes, causing the development of a temperature anomaly below, which in turn reduces the buoyancy and weakens the AMOC. The formation of a surface cap does not qualitatively alter the rate of AMOC weakening, and the AMOC weakening was not found to be sensitive to whether the weakening is dominated by salinity or temperature changes.

Acknowledgements This project was funded by a NERC Industrial CASE studentship in partnership with the Met Office (NE/M010295/1). We would like to thank Robin Smith and Jeff Blundell for their support and guidance in the running of FAMOUS.

Open Access This article is distributed under the terms of the Creative Commons Attribution 4.0 International License (<http://creativecommons.org/licenses/by/4.0/>), which permits unrestricted use, distribution, and reproduction in any medium, provided you give appropriate credit to the original author(s) and the source, provide a link to the Creative Commons license, and indicate if changes were made.

References

- Bakker P, Schmittner A, Lenaerts JTM, Abe-Ouchi A, Bi D, Broecker MR, Chan W-L, Hu A, Beadling RL, Marsland SJ, Mernild SH, Saenko OA, Swingedouw D, Sullivan A, Yin J (2016) Fate of the Atlantic meridional overturning circulation—strong decline under continued warming and Greenland melting. *Geophys Res Lett* 43(23):12252–12260. <https://doi.org/10.1002/2016GL070457>
- Bouttes N, Good P, Gregory JM, Lowe JA (2015) Non-linearity of ocean heat uptake during warming and cooling in the FAMOUS climate model. *Geophys Res Lett* 42:2409–2416
- Bryan F (1987) Parameter sensitivity of primitive equation ocean general circulation models. *J Phys Oceanogr* 17:970–985
- Butler ED, Oliver KIC, Hirschi JJM, Mecking JV (2016) Reconstructing global overturning from meridional density gradients. *Clim Dyn* 46(7–8):2593–2610. <https://doi.org/10.1007/s00382-015-2719-6>
- Cimatoribus AA, Drijfhout SS, Dijkstra HA (2014) Meridional overturning circulation: stability and ocean feedbacks in a box model. *Clim Dyn*. <https://doi.org/10.1007/s00382-012-1576-9>
- de Boer AM, Gnanadesikan A, Edwards NR, Watson AJ (2010) Meridional density gradients do not control the Atlantic overturning circulation. *J Phys Oceanogr* 40(2):368–380. <https://doi.org/10.1175/2009JPO4200.1>
- Gent PR, McWilliams JC (1990) Isopycnal mixing in ocean circulation models. *J Phys Oceanogr* 20(1):150–155
- Gordon C, Cooper C, Senior CA, Banks H, Gregory JM, Johns TC, Mitchell JFB, Wood RA (2000) The simulation of SST, sea ice extents and ocean heat transports in a version of the hadley centre coupled model without flux adjustments. *Clim Dyn* 16:147–168
- Haskins RK, Oliver KIC, Jackson LC, Drijfhout SS, Wood RA (2019) Explaining asymmetry between weakening and recovery of the AMOC in a coupled climate model. *Clim Dyn* 53(1):67–79. <https://doi.org/10.1007/s00382-018-4570-z>
- Hawkins E, Smith RS, Allison LC, Gregory JM, Woollings TJ, Pohlmann H, De Cuevas B (2011) Bistability of the Atlantic overturning circulation in a global climate model and links to ocean

- freshwater transport. *Geophys Res Lett* 38(10):1–6. <https://doi.org/10.1029/2011GL047208>
- Henry LG, Henry LG, McManus JF, Curry WB, Roberts NL, Piotrowski AM, Keigwin LD (2016) North Atlantic ocean circulation and abrupt climate change during the last glaciation. *Science* 352(6):470–474. <https://doi.org/10.1126/science.aaf5529>
- Jackson LC (2013) Shutdown and recovery of the AMOC in a coupled global climate model: the role of the advective feedback. *Geophys Res Lett* 40(6):1182–1188. <https://doi.org/10.1002/grl.50289>
- Jackson LC, Wood RA (2018) Timescales of AMOC decline in response to fresh water forcing. *Clim Dyn* 51(4):1333–1350. <https://doi.org/10.1007/s00382-017-3957-6>
- Jackson LC, Smith RS, Wood RA (2017) Ocean and atmosphere feedbacks affecting AMOC hysteresis in a GCM. *Clim Dyn* 49:173–191. <https://doi.org/10.1007/s00382-016-3336-8>
- Krebs U, Timmermann A (2007) Tropical air-sea interactions accelerate the recovery of the Atlantic meridional overturning circulation after a major shutdown. *J Clim* 20(19):4940–4956. <https://doi.org/10.1175/JCLI4296.1>
- Marotzke J (1997) Boundary mixing and the dynamics of three-dimensional thermohaline circulations. *J Phys Oceanogr* 27:1713–1728
- McManus JF, Francois R, Gherardi J-M, Keigwin LD, Brown-Leger S (2004) Collapse and rapid resumption of Atlantic meridional circulation linked to deglacial climate changes. *Nature* 428(6985):834–837. <https://doi.org/10.1038/nature02494>
- Megann A, Storkey D, Aksenov Y, Alderson S, Calvert D, Graham T, Hyder P, Siddorn J, Sinha B (2014) GO5.0: the joint NERCMet office NEMO global ocean model for use in coupled and forced applications. *Geosci Model Dev* 7(3):1069–1092. <https://doi.org/10.5194/gmd-7-1069-2014>
- Mignot J, Ganopolski A, Levermann A (2007) Atlantic subsurface temperatures: response to a shutdown of the overturning circulation and consequences for its recovery. *J Clim* 20(19):4884–4898. <https://doi.org/10.1175/JCLI4280.1>
- Oliver KIC, Watson AJ, Stevens DP (2005) Can limited ocean mixing buffer rapid climate change? *Tellus Ser A* 57(4):676–690. <https://doi.org/10.1111/j.1600-0870.2005.00119.x>
- Robinson AR (1960) The general thermal circulation in equatorial regions. *Deep-Sea Res* 6:311–317
- Sévellec F, Huck T (2016) Geostrophic closure of the zonally averaged Atlantic meridional overturning circulation. *J Phys Oceanogr* 46(3):895–917. <https://doi.org/10.1175/JPO-D-14-0148.1>
- Sijp WP, Gregory JM, Tailleux R, Spence P (2012) The key role of the western boundary in linking the AMOC strength to the north-south pressure gradient. *J Phys Oceanogr* 42:628–643. <https://doi.org/10.1175/JPO-D-11-0113.1>
- Smith RS (2012) The FAMOUS climate model (versions XFXWB and XFHCC): description update to version XDBUA. *Geosci Model Dev* 5(1):269–276. <https://doi.org/10.5194/gmd-5-269-2012>
- Smith RS, Gregory JM, Osprey A (2008) A description of the FAMOUS (version XDBUA) climate model and control run. *Geosci Model Dev* 1(1):53–68. <https://doi.org/10.5194/gmd-1-53-2008>
- Stouffer RJ, Yin J, Gregory JM, Dixon KW, Spelman MJ, Hurlin W, Weaver AJ, Eby M, Flato GM, Hasumi H, Hu A, JungCLAUS JH, Kamenkovich IV, Levermann A, Montoya M, Murakami S, Nawrath S, Oka A, Peltier WR, Robitaille DY, Sokolov A, Vettoretti G, Weber SL (2006) Investigating the causes of the response of the thermohaline circulation to past and future climate changes. *J Clim* 19:1365–1387. <https://doi.org/10.1175/jcli3689.1>
- Swingedouw D, Braconnot P (2007) Effect of the Greenland ice-sheet melting on the response and stability of the AMOC in the next centuries. American Geophysical Union Geophysical Monograph Series, Washington DC, pp 383–392
- Thorpe RB, Gregory JM, Johns TC, Wood RA, Mitchell JFB (2001) Mechanisms determining the Atlantic thermohaline circulation response to greenhouse gas forcing in a non-adjusted coupled climate model. *J Clim* 14:3102–3116. [https://doi.org/10.1175/1520-0442\(2001\)014%3c3102:MDTATC%3e2.0.CO;2](https://doi.org/10.1175/1520-0442(2001)014%3c3102:MDTATC%3e2.0.CO;2)
- Williams KD, Harris CM, Camp J, Comer RE, Copsey D, Fereday D, Graham T, Hill R, Hinton T, Hyder P, Ineson S, Masato G, Milton SF, Roberts MJ, Rowell DP, Sanchez C, Shelly A, Sinha B, Walters DN, West A, Woollings T, Xavier PK (2015) The met office global coupled model 2.0 (GC2) configuration. *Geosci Model Dev* 88:1509–1524. <https://doi.org/10.5194/gmd-88-1509-2015>
- Wu P, Jackson L, Pardaens A, Schaller N (2011) Extended warming of the northern high latitudes due to an overshoot of the Atlantic meridional overturning circulation. *Geophys Res Lett* 38:L24704. <https://doi.org/10.1029/2011GL049998>

Publisher's Note Springer Nature remains neutral with regard to jurisdictional claims in published maps and institutional affiliations.